

## ON THE IMPROVED NOTCH SHAPE

Daniel de Albuquerque Simões, dsimoes3@gmail.com

Jaime Tupiassú Pinho de Castro, jtcastro@puc-rio.br

Marco Antonio Meggiolaro, meggi@puc-rio.br

Mechanical Engineering Department, PUC-Rio

**Abstract.** *Most structural components have notches, or geometric transition details such as holes, slots, grooves, keyways, shoulders, corners, threads, weld chords, reinforcements, etc., which are required to fix and/or to operate them. These notches locally concentrate (increase) the nominal stresses that would act in their location, if they were not there. Stress concentration effects are of primordial importance in many failure mechanisms, such as fatigue crack initiation or fracture of brittle components, and must be accounted for in structural analysis. However, the usual constant radius notch tip roots, used in most structural members to alleviate their stress concentration effects, do not minimize them. In fact, natural structural members, such as tree branches and bones, after many million years of evolution have learned to use variable tip radii instead of the fixed radius typical of engineering notches. This problem has been recognized for a long time, but variable radius notches optimized to minimize their deleterious influence on fatigue strength still are not widely used in mechanical design. The usual practice is to specify notches with as large as possible constant radius roots, since they can be easily fabricated in traditional machine tools. However, notches with properly specified variable radius can have much lower stress concentration factors than those obtainable by fixed notch root radii. Therefore, such improved notches can be a good design option to augment fatigue lives without significantly affecting structural components global dimensions and weight. Moreover, these improved notches are certainly more useful than ever, as nowadays they can be economically specified and manufactured in many structural components, due to the wide availability of CNC machine tools. This paper quantifies the stress concentration improvements achievable by two variable radius notches traditional receipts, and presents a numerical routine developed to improve notch shapes for components which work under the general multiaxial loading case.*

**Keywords:** *Structural components, stress concentration, variable radius notches, fatigue life improvement*

### 1. INTRODUCTION

Notches are geometric details such as holes, slots, grooves, keyways, shoulders, corners, and threads, inevitably found in structural components. Despite being necessary for their functionality, such details locally change the stress distribution increasing, or concentrating, the nominal stresses around their roots. This effect is quantified by the notch stress concentration factor (SCF)  $K_t = \sigma_{max}/\sigma_n$ , where  $\sigma_{max}$  is the maximum stress at its root and  $\sigma_n$  is the nominal stress which would act there if the notch had no effect on the stress distribution. High  $K_t$  values can have a very deleterious effect on failure mechanisms such as fatigue crack initiation and brittle fracture. To mitigate such effects, abrupt geometrical transitions should be avoided, in particular by seeking to smooth notch tip roots. Designers commonly use circular profiles to do so.  $K_t$  values for these standard profiles may be conveniently obtained from the literature (see Pilkey 1997, e.g.), but they might not be the best choice to minimize deleterious notch effects.

For example, instead of being constant, the notch tip curvature may be numerically optimized to reach a uniform tangential stress along at least part of the curve boundary. An optimization algorithm, such as the so-called gradientless algorithm, may be used to iteratively add material where the stresses are high and to remove it where the stresses are too low (Heller et al, 1999, Waldman et al, 2000, Taylor et al, 2010). In fact, variable radii notches may be often found in old cast components. Apparently, old machine designers intuitively designed using variable radius instead of a constant one. In recent days, the shape of trees inspired Mattheck (1990, 2006) to better understand how nature biologically improves their roots, barks and branches. He showed that this concept could be also applied to mechanical components. Much earlier Grodzinski in 1941 (Pilkey, 1997) developed a simple purely graphical method for creating a variable radius curve that may also lead to lower  $K_t$  than the circular traditional profile. Despite its simplicity, this variable curve concept has been neglected by most modern designers. However, these two methodologies, if correctly applied, can considerably reduce stress concentration effects at notch roots, and therefore, increase the fatigue life of structural components, leading to very significant economic savings.

The purpose of this paper is to systematically compare Mattheck and Grodzinkis' notch root shapes against the traditional constant radius profile using 2D finite element analysis, to quantify how they behave when subjected to tension and bending loads.

### 2. QUANTIFICATION OF THE STRESS CONCENTRATION FACTOR

Some few stress concentration factors can be analytically calculated using Theory of Elasticity concepts. Kirsh's solution for the circular hole in an infinite plate under pure tension, which induces a  $K_t = 3$ , is relatively simple to reproduce. Inglis' elliptical hole SCF in an infinite plate is also well known in its simplest version, the plate under pure ten-

sion perpendicular to the ellipsis semi-axis  $a$ : its  $K_t = 1 + 2a/b = 1 + 2\sqrt{a/\rho}$ , where  $b$  is the other semi-axis of the elliptical hole, which has a tip radius  $\rho = b^2/a$ . This classical formula illustrates why sharp notches are inadmissible in mechanical design, and justifies the need to increase notch tip radii, but the Inglis' plate general solution is much more involved. More complex geometries are not analytically treatable, and most  $K_t$  values listed in classical handbooks (Pilkey, 1997) were experimentally measured, usually by photoelastic techniques.

Some classical approximations may be useful to deal with unlisted geometries. For example, in absence of better information, McClintock says that  $K_t$  can be estimated to be in the range  $1 + 0.5\sqrt{a/\rho} \leq K_t \leq 1 + 2\sqrt{a/\rho}$  for most geometries, with  $a$  and  $\rho$  defined in Fig. 1. Higher  $K_t \cong 1 + 2\sqrt{a/\rho}$  values should be used for shallow severe notches ( $\rho$  and  $a \ll D$ ) with parallel faces under tension. Smaller  $K_t$  values,  $K_t \cong 1 + 0.5\sqrt{a/\rho}$ , are appropriate for gentler notches, with large tip radius and face angle, under bending or torsion loads. The range 0.5 to 2 is quite large, and the notch severity is subjectively judged, but a crude estimate is better than no estimate at all (Castro and Meggiolaro, 2009).

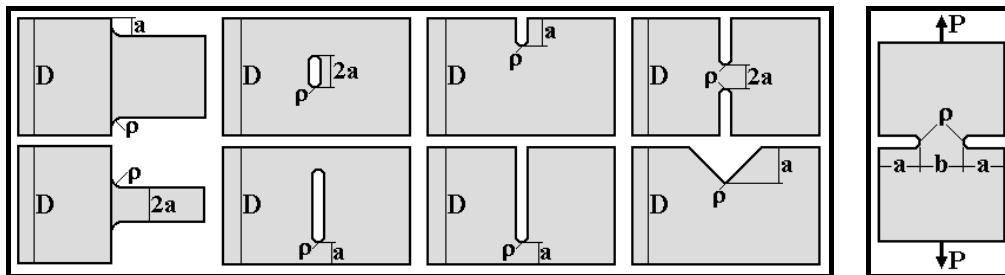


Fig 1: Characteristic dimensions used in McClintock's estimate, and double U-notches for Neuber estimate.

According to Neuber, SCF  $K_{ts}$  for shallow notches, with depth much smaller than their residual ligaments, can be estimated by the Inglis formula  $K_{ts} \cong 1 + 2\sqrt{a/\rho}$ , where  $\rho$  is the notch tip radius and  $a$  is its depth or length. SCF for deep notches  $K_{td}$ , on the other hand, depends on  $\rho$  and on  $b$ , the residual ligament size, and can be estimated by:

$$K_{td} \cong \left\{ 2\sqrt{b/2\rho} \cdot [(b/2\rho) + 1] \right\} / \left\{ [(b/2\rho) + 1] \operatorname{atan} \sqrt{b/2\rho} + \sqrt{b/2\rho} \right\} \quad (1)$$

The  $K_t$  for any notch, large or small, can be estimated from  $K_{ts}$  and  $K_{td}$  by:

$$K_t \cong 1 + (K_{td} - 1) \cdot (K_{ts} - 1) / \sqrt{(K_{td} - 1)^2 + (K_{ts} - 1)^2} \quad (2)$$

This estimate was developed for plates with two U notches loaded in mode I, see Fig. 1, but it can be used to estimate  $K_t$  values for several other geometries. The double U notches have parallel sides, but V notches with angles up to about  $90^\circ$  in plates or  $60^\circ$  in shafts induce  $K_t$  values just a bit smaller than the U notches. These estimates assume that the nominal stress  $\sigma_n$  acts in the residual ligament, or in the liquid area (Castro and Meggiolaro, 2009).

Creager and Paris (1967) proposed a way to estimate notch SCF  $K_t$  from the stress intensity factors (SIF)  $K_I$  of cracks geometrically similar to them. They showed that LE stress fields around elongated notches with tip radius  $\rho$  can be estimated from the corresponding cracks  $K_I$ -controlled stress fields (when loaded in mode I), if the coordinated axis  $r$  and  $\theta$  origin is moved to  $\rho/2$  inside the notch, see Fig. 2. This is no surprise, since notches are similar to blunt cracks, or to cracks with rounded tips, which radii  $\rho \neq 0$ . In this way,  $K_t$  for notches loaded in mode I can be estimated by:

$$K_t \cong 2K_I / \left[ \sigma_n \sqrt{\pi\rho} \right] \quad (3)$$

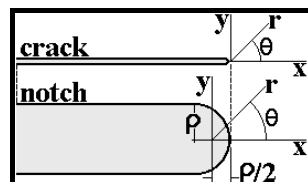


Fig. 2: Coordinates used in Creager and Paris' model.

However, nowadays complex linear elastic stress concentration problems can be conveniently tackled using standard finite element (FE) procedures. FE is a global method of analysis which calculates the whole displacement, strain, and/or stress fields in structural components, using a proper mesh to subdivide them in small parts (or finite elements,) and then forcing the FE to remain compatible after the loading (Bathe 1982). But it is worthwhile to mention that in  $K_t$  calculations by FE, the mesh around the notch root must be properly refined, using elements much smaller than its radius  $\rho$ , to resolve the local stresses. It is interesting to compare such estimates with the FE solution for a non-elementary SCF problem, an un-cracked C(T) specimen shown in Fig. 3 (Castro and Meggiolaro, 2009).

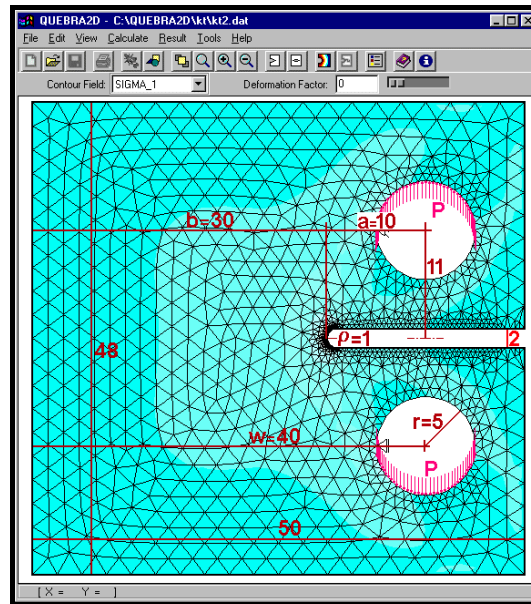


Fig. 3: C(T) specimen, with a blunt notch of length  $a = 10\text{mm}$  and tip radius  $\rho = 1\text{mm}$ .

A powerful numerical tool specially developed to model by FE fatigue crack propagation problems in arbitrary two-dimensional (2D) geometries, named **Quebra2D** was used in this calculation. This program automatically calculates  $K_I$  and  $K_{II}$  and the generally curved crack paths using special quarter point crack tip elements, appropriated criteria to predict the crack increment direction, robust and efficient auto-adaptative remeshing algorithms, and a friendly interface (Miranda et al, 2003). Fig. 3 shows the mesh used in this analysis. Note its refinement around the notch tip (the mesh must be subdivided there until the value of  $\sigma_{max}$  calculated at the notch tip converges.) The calculated SCF in this case is  $K_t = 4.78$ , considering that the nominal stress (which would act there if the notch did not affect the stress field around the notch tip) is defined by the sum of the tensile and bending stresses given by:

$$\sigma_n = \sigma_{nN} + \sigma_{nM} = P/bt + 6P(a+b/2)/tb^2 \quad (4)$$

Assuming FE calculations can be used as a reference, McClintock estimation  $K_t \cong 1 + \alpha \cdot \sqrt{a/\rho}$ , with  $0.5 \leq \alpha \leq 2$ , for this C(T) notch has  $\alpha = 1.20$ . This non-intuitive value is due to the bending predominance, which tends to reduce the estimation parameter  $\alpha$ . The Neuber estimate, using  $a = 10$ ,  $b = 30$  and  $\rho = 1$ , is given by:

$$\begin{cases} K_{t_s} \cong 1 + 2\sqrt{a/\rho} = 7.32 \\ K_{t_d} \cong \frac{2\sqrt{\frac{b}{2\rho}} \cdot \left[\frac{b}{2\rho} + 1\right]}{\left[\frac{b}{2\rho} + 1\right] \cdot \text{atan}\sqrt{\frac{b}{2\rho}} + \sqrt{\frac{b}{2\rho}}} = 4.96 \end{cases} \Rightarrow K_t \cong 1 + \frac{(K_{t_d} - 1) \cdot (K_{t_s} - 1)}{\sqrt{(K_{t_d} - 1)^2 + (K_{t_s} - 1)^2}} = 4.36 \quad (5)$$

Compared to FE,  $K_t$  is underestimated by Neuber in about 9%, a non-conservative result, and overestimated by  $K_{t_d}$  in about 4%, a smaller and conservative error. By Creager and Paris, using the C(T)  $K_I$ , the estimated  $K_t$  is:

$$\begin{cases} K_I = \frac{P}{t\sqrt{40}} \frac{2+1/4}{(1-1/4)^{1.5}} \left[ 0.886 + 4.64\left(\frac{1}{4}\right) - 13.3\left(\frac{1}{4}\right)^2 + 14.7\left(\frac{1}{4}\right)^3 - 5.6\left(\frac{1}{4}\right)^4 \right] = 0.78 \frac{P}{t} \Rightarrow \\ K_t \cong \frac{2K_I}{\sigma_n \cdot \sqrt{\pi\rho}} = \frac{2 \cdot 0.78 \cdot P/t}{(0.2P/t) \cdot \sqrt{\pi \cdot 1}} = 4.40 \end{cases} \quad (6)$$

Thus, when compared with the FE solution, the C(T)  $K_t$  is underestimated in nearly 8%, confirming that Creager and Paris is useful, but must be used with care. These interesting comparisons are useful and representative, but they cannot, of course, be generalized for all practical cases.

### 3. VARIABLE RADII NOTCHES

Mattheck noticed that nature does not use constant radii notches, and found a smarter way to improve the structural integrity of the trees. He observed that organic material grows where the stress concentrates in the tree structure, as illustrated in Fig. 4.

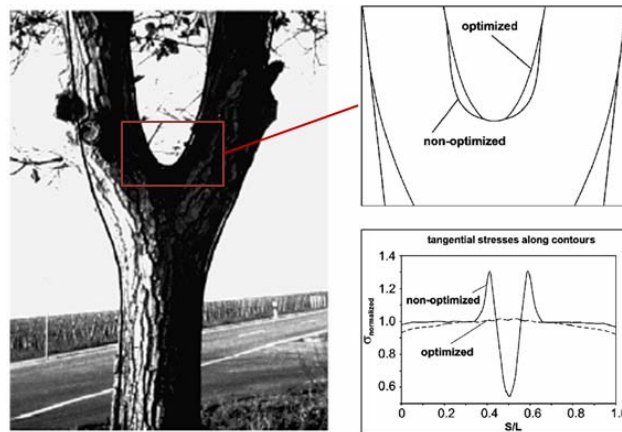


Fig. 4: Tree geometry optimization (Mattheck 2006, modified)

Mattheck proposed to apply these concepts nature to actual mechanical components. He developed a simple, but efficient graphical way of creating variable radius fillets, called the method of tensile triangles, see figure 5.

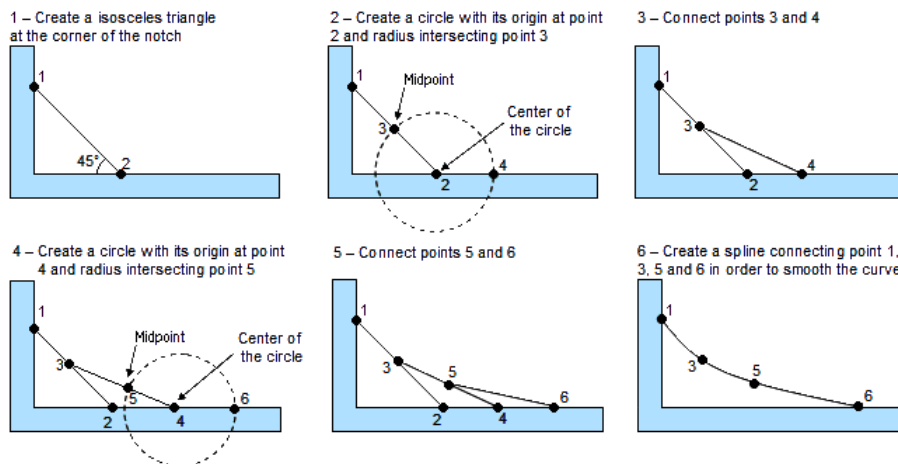


Fig. 5: Mattheck's tensile triangle method

Grodzinski proposed another graphical method of creating a variable radius curve, by dividing the available space for the fillet in the same number of equally spaced intervals and connecting them by straight lines, as shown in figure 6.

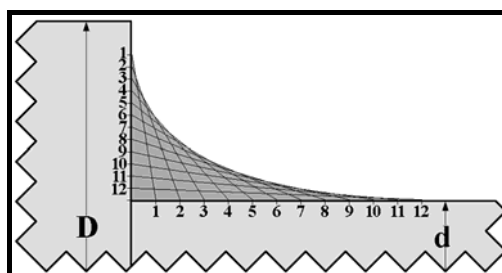


Fig. 6: Grodzinski's variable radius curve

Both methods use graphically generated curves. Nevertheless, these improved fillet profiles significantly reduce  $K_t$  values. A few decades ago it would not be feasible to automatically generate and analyze such graphically generated variable fillets, but CAE/CAM tools are becoming more and more available, and manufacturing a component with variable curve exactly as specified by the designer is nowadays a simple task. Therefore, the designer has at his/her disposal three quick ways of smoothing sharp edges without any calculation whatsoever: the circular, Mattheck, and Grodzinski's fillets, see fig. 7. In addition to the difference of the curve profiles, it is clearly seen that these curves also differ in their geometry size along the  $x$  and  $y$  direction. Fortunately, one of the advantages of these geometrical method is that these curve may be easily scaled up or down according to meet the geometrical limitations, such as interference with other components (e.g. roller bearings) during its assembly.

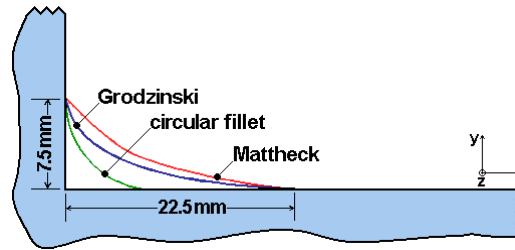


Fig. 7: Geometrical profiles for constant radius, Mattheck, and Grodzinski fillets.

Figure 8 shows a hypothetical flat bar subjected to a remote pure tension loading of 10 kN along the edges. As it may be seen, its shoulder has an abrupt change in geometry that would lead to severe stress concentration effects around its root, which must be avoided by properly smoothing its profile.

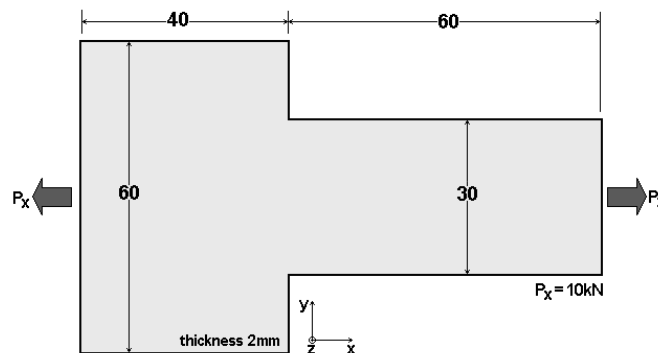


Fig. 8: Flat bar subjected to tension loading

The designer must specify an appropriate curve to smooth out this notch root geometry. The challenge is to take into account not only the stress concentration reduction but also the geometric constrains. Depending on the application of the component, the extension of the smoothing curve along the shoulder may be limited. This geometry was modeled in a standard commercial finite element software, to study the effect of three different notch root smoothing curves effectiveness: constant radius, Mattheck and Grodzinski.

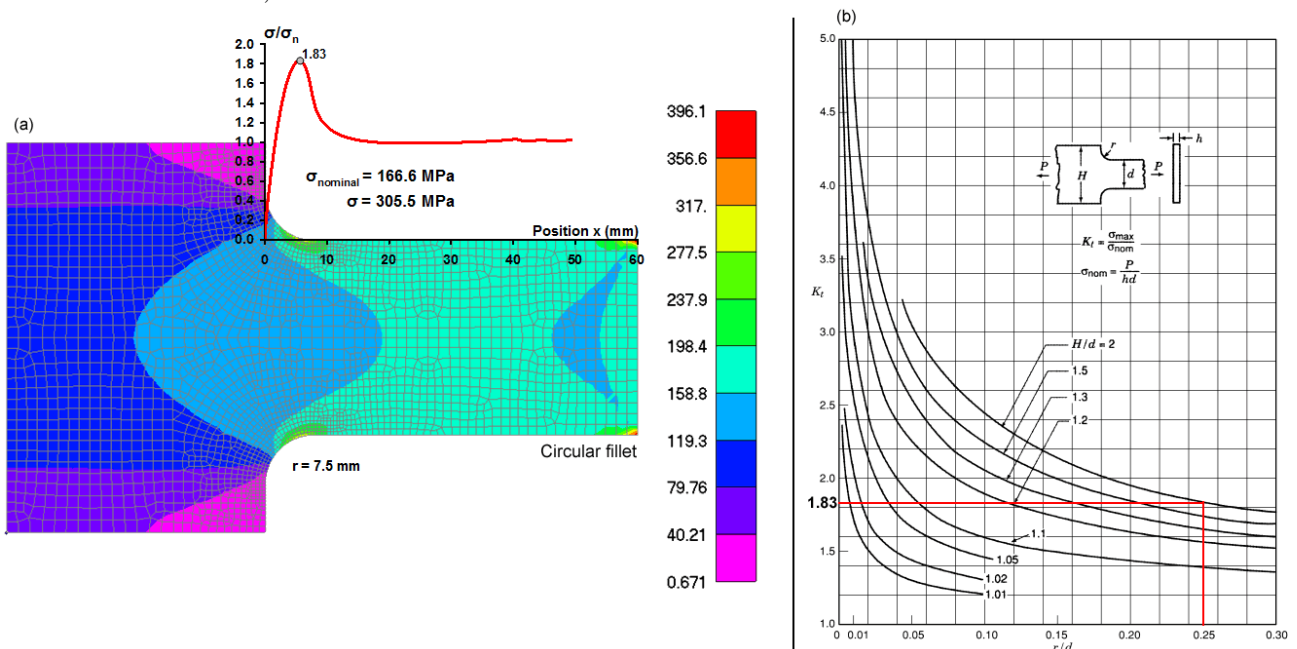


Fig. 9: Constant radius geometry - Finite element plot for von Mises stress (a) and Peterson's curve (b) for stress concentration factor of a flat tension bar with shoulder fillet (modified)

When the notch is smoothed with a shoulder fillet of constant radius, the stress concentration factor, obtained from the finite element analysis, is approximately 1.83. This value is corroborated by Peterson's chart for a flat tension bar with shoulder fillet. Figure 10 shows the stress plot results for von Mises stress and the stress concentration variation along the curve profile for Mattheck's and Grodzinski's curve respectively.

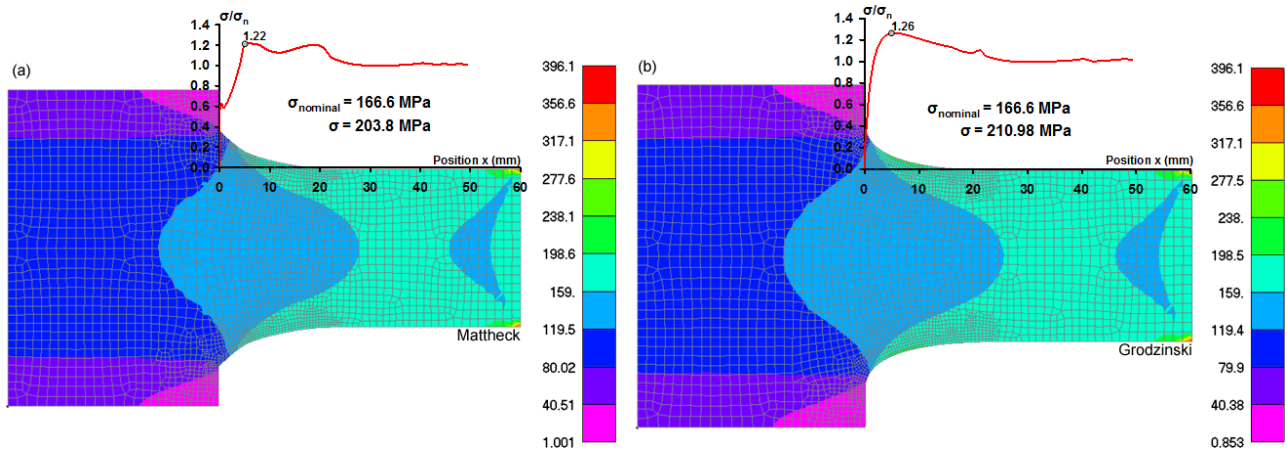


Fig. 10: Mattheck (a) and Grodzinski's (b) variable radius geometry fillets under tensile loading.

Figure 11 shows a comparison of the stress concentration effect calculated along the bar upper edge for the constant tip radius notch, and for the Mattheck and Grodzinski's improved notch profiles. Their stress concentration factors are, respectively, 1.83, 1.22, and 1.26. Thus, the ratio between the SCF  $K_t$  induced by the traditional circular profile and the one associated to the Grodzinski's curve is approximately 1.45, and between the circular profile and Mattheck's curve is about 1.5, demonstrating that they do introduce an improvement that is certainly far from negligible.

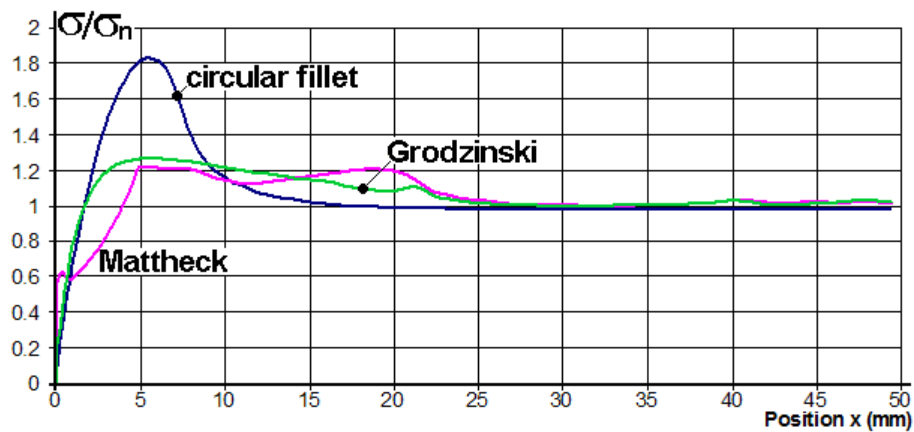


Fig.: 11.  $K_t$  for the constant radius, Mattheck's and Grodzinski's curve for a flat be under pure tension loading

Let the same hypothetical component be now subjected to a remote pure bending load in its plane, as sketched in figure 12.

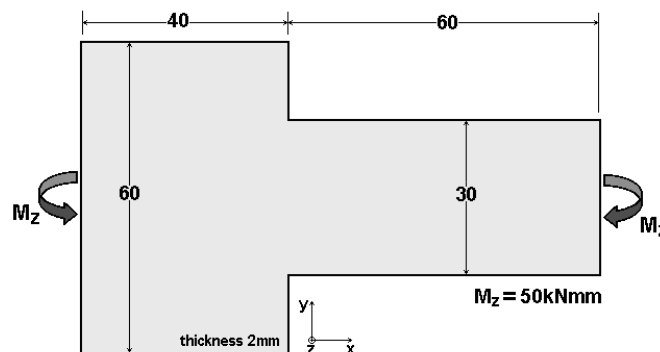


Fig. 12: Hypothetical geometry

When the notch root is smoothed with a constant radius fillet, this shoulder SCF, obtained from this bent plate FE analysis, is approximately 1.46. This value is also corroborated by Peterson's chart for a flat bar with shoulder fillet under such a bending load, see figure 13.



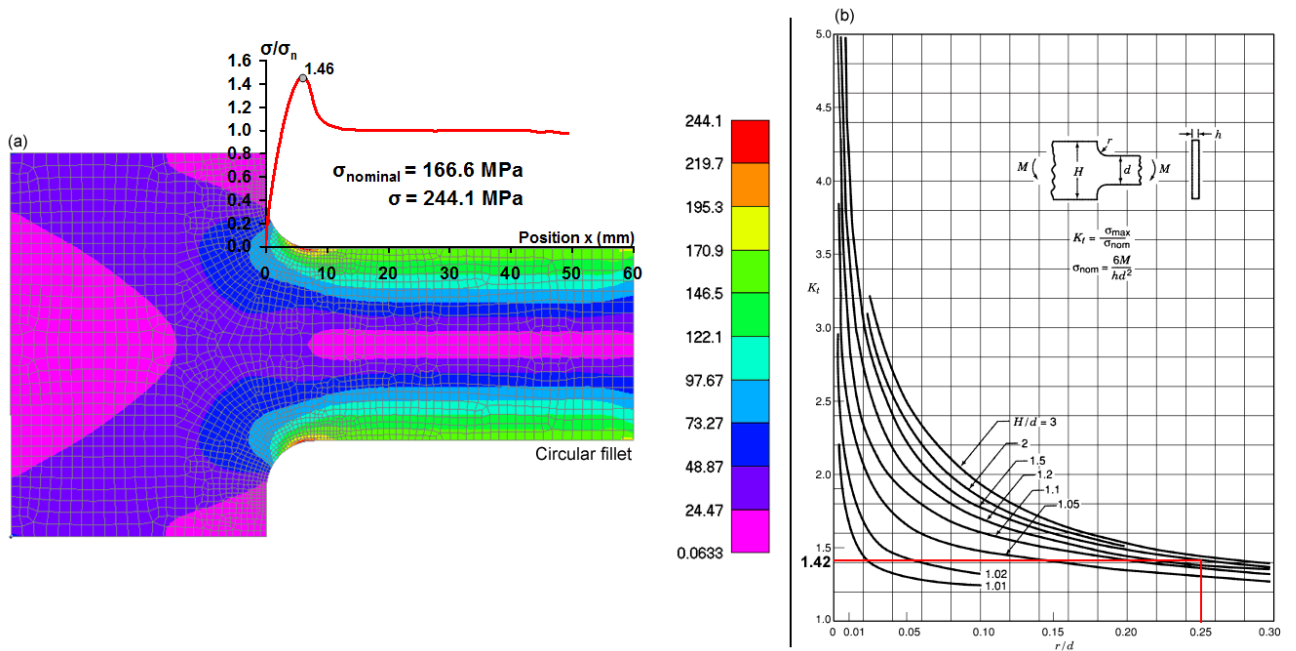


Fig. 13: Constant radius geometry - Finite element plot for the Mises stress distribution (a) and (b) Peterson's curve for the stress concentration of flat bars with fixed radii shoulder fillets bent in their own plane.

Figure 14 show the Mises stress fields in the whole plates, and the stress concentration effect along the plates upper edges, described by their  $\sigma/\sigma_n$  ratio departing from the fillet profile starting point, for the plates with improved notches designed following Mattheck's and Grodzinski's receipts, loaded by pure in plane bending moments. It is important to emphasize that such plates, as well as the plates illustrated in figure 10, have notch root profiles with same end points, as depicted in figure 7. Moreover, their notches roots have the same 7.5 mm height of the circular tip studied in figures 9 and 13. In this way, the improvement introduced by the variable root radii notches can be reasonably well compared. Even thou these simple smoothing receipts do not optimize the notch profile, in the sense of minimizing their  $K_t$  values, they are remarkably efficient, and should not be ignored by structural designers.

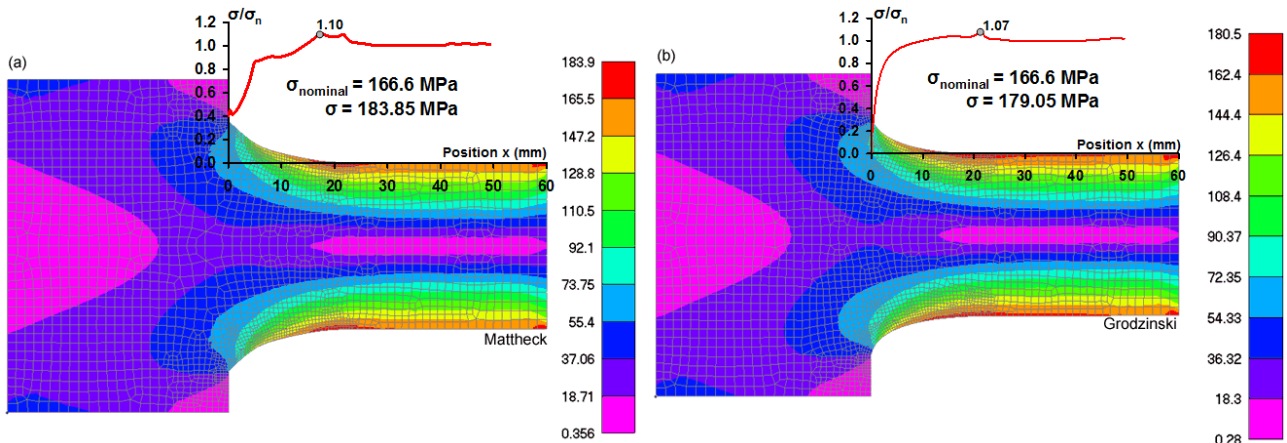


Fig. 14: Plate with (a) Mattheck and (b) Grodzinski's shoulder fillets with variable radius geometries under in plane bending loads, and their respective  $K_t$  values calculated by FE.

Figure 15 compares the three Mises to nominal stress  $\sigma/\sigma_n$  ratios, calculated along the plates upper edges for the shoulders with constant radius, Mattheck and Grodzinski's profiles, as shown in figures 13 and 14. Their SCF are, respectively,  $K_t = 1.46$ ,  $K_t = 1.10$ , and  $K_t = 1.07$ . The ratio between the SCF introduced by traditional circular notch root and the Grodzinski's variable radius profile is approximately 1.36, whereas the ratio between the fixed radius and the Mattheck SCF is about 1.33.

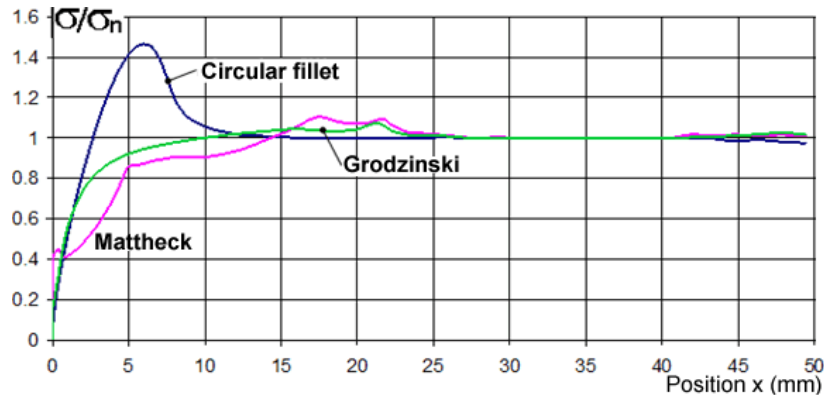


Fig. 15:  $K_t$  for the constant radius, Mattheck's and Grodzinski's curve for a flat be under pure bending loading

A more practical example further illustrates these variable notch radii profiles potential. Offshore structures, for instance, FPSO and semisubmersible platforms, contain innumerable plate-like components with openings, frequently used to reinforce girders and other structural members. An inspection window cut-out on a steel plate may be used as a good example of such components. This hole concentrates stresses around its corners, from where fatigue cracks can depart and eventually lead the structure to ruin. Keeping this in mind, the designer is challenged to specify an adequate geometry to reduce the stress concentration there. In order to illustrate the behavior of this discontinuity, figure 16 shows a generic example of an inspection window cutout on a plate subjected to a generic constant remote pure tension load.

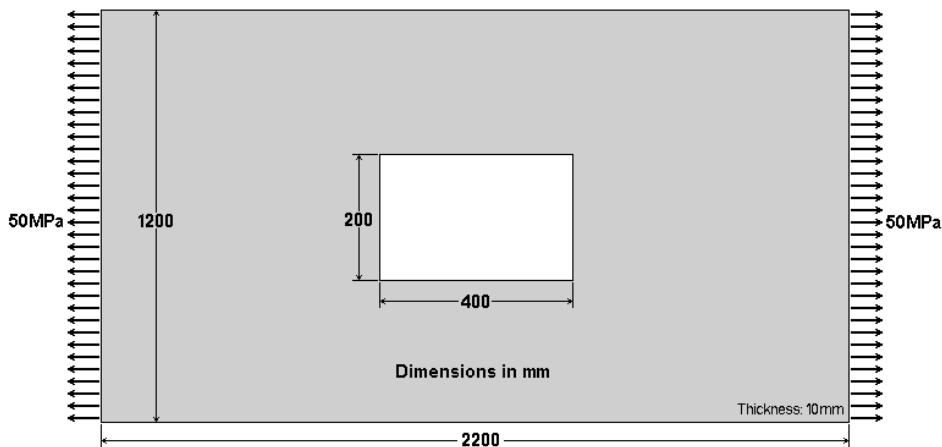


Fig. 16: Example of an inspection window cutout subject to pure tension loading

The corners of this inspection window may be smoothed out by a circular fillet or by a variable radius curve, following, e.g., Mattheck's receipt, see figure 17. It is important to note that a spline is adjusted to Mattheck's points, to smooth out the corner profile.

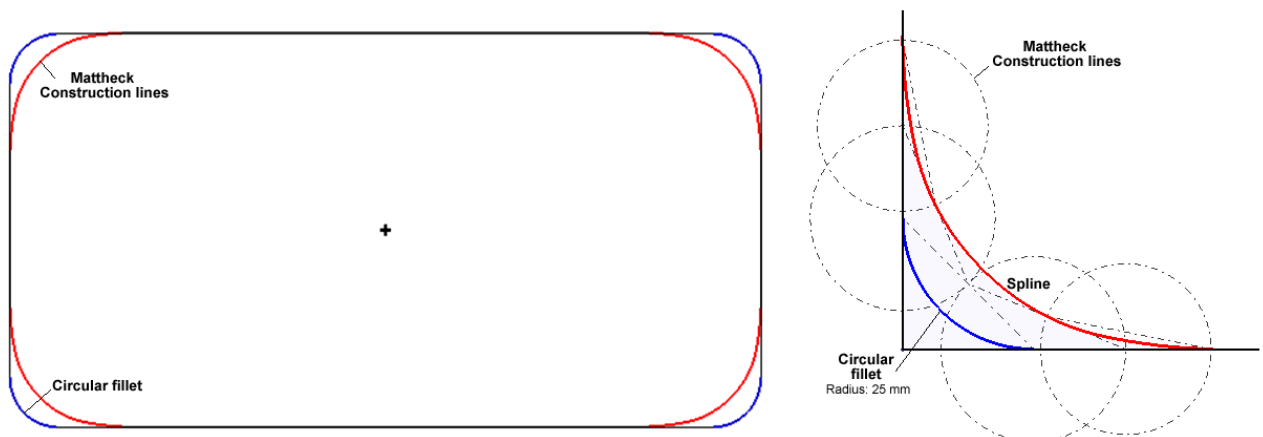


Fig. 17: Comparison between Mattheck and Grodzinski's smoothing curves



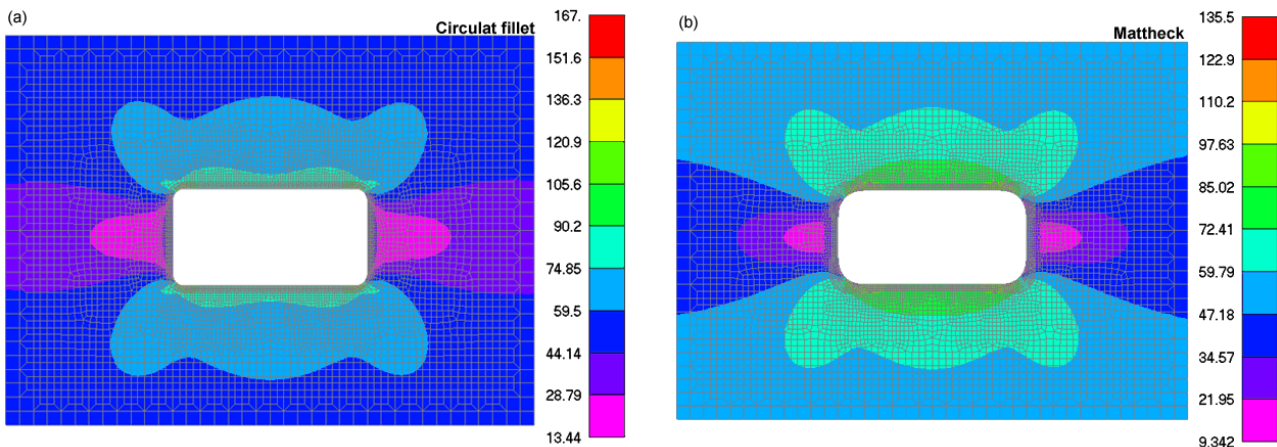


Fig. 18: von Mises stress plot for Mattheck (a) and Grodzinski's (b) geometry for an illustrative inspection window subjected to pure tension loading

The Mises stress around the inspection window cutout for both the constant and variable radius were extracted from the finite element model analysis results and are plotted in the same chart, to aid the comparison between them. The stress calculation starts in the node indicated in figure 19 and proceeds counterclockwise along the cutout edge. The stress reduction obtained by the variable curve is approximately 19% lower than the obtained by the constant one.

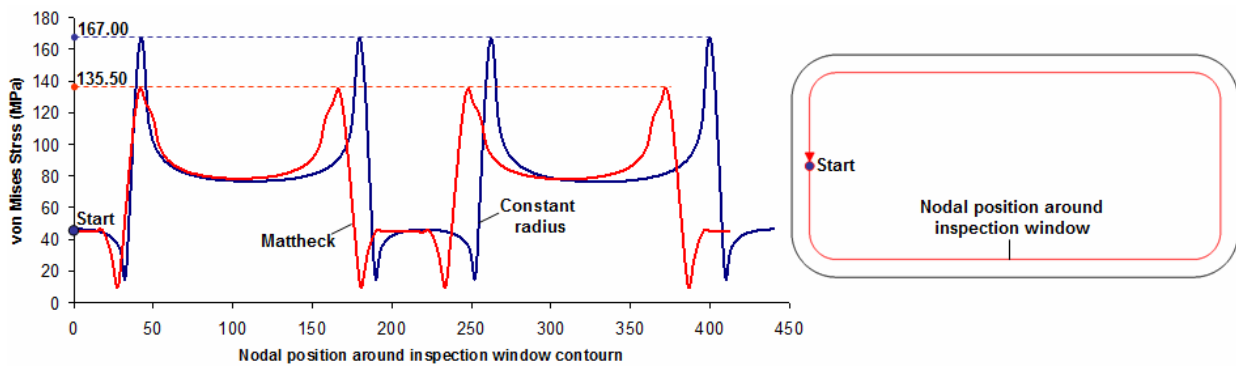


Fig. 19: Example of an inspection window cutout subject to pure tension loading

The purpose of this example is to enhance the considerable SCF reduction that can be achieved with such little effort. It is important to point out, though, that this is not the optimum solution for this problem. It is rather an improved solution based on heuristic geometrical models. However, this methodology is quite useful for those who need a quick and efficient solution to improve the geometry and minimize the stress concentration problem. For instance, this geometrical improvement could be easily employed in the early stages of the component design, and also when reworking an existing one by reshaping its geometry to a more suitable profile in order to considerably extend its fatigue life. Moreover, it may also be used to remove highly stressed material, in which fatigue damage may have accumulated.

However, if the designer wants to obtain the optimum solution for the root profile (the “best” curve that uniform the tangential stress and, consequently, minimizes the stress concentration,) he/she should use an optimization shape procedure, such as the gradientless algorithm, see for example, Heller *et al.* (1999) and Waldman and Heller (2000).

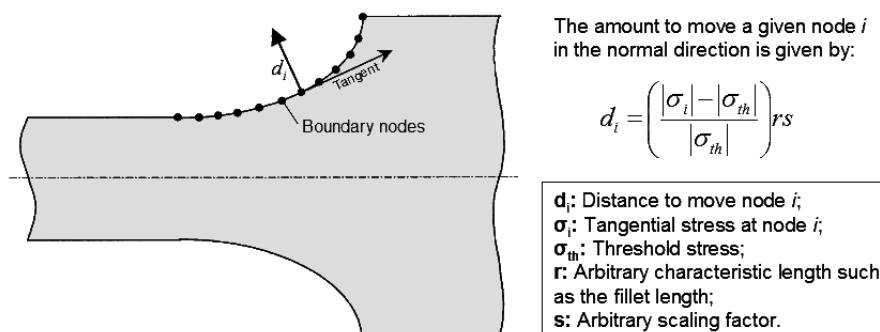


Fig. 20: Gradientless shape optimization method in a loaded plate. Waldman and Heller (Modified)

To summarize, the gradientless method seeks a constant boundary tangential stress by iteratively moving the fillet curve boundary nodes an amount proportional to the tangential stress obtained in a previous analysis, until the uniform tangential stress along the curvature is achieved. This methodology basically follows the same rule that Mattheck proposed: add material where the stress is high, and remove it where the stress is low.

### 3. CONCLUSIONS

Fatigue is one of the most common fracture mechanisms that may occur during the life time of structural components subjected to cycling loading. Fatigue failures initiate at the spot where the stress is higher, that is, almost always at notch roots, where the nominal stress is highly increased by their geometrical discontinuities. Fortunately, there are efficient ways of reducing such stress concentration by smoothing out sharp notches. The notch may be smoothed out by finding a geometry that seeks a uniform tangential stress along its root profile. On the one hand, this geometry may be much improved by simple curves such as those proposed by Mattheck and Grodzinski, which do not result in the optimum solution for this problem, but nevertheless result in much smaller stress concentration effects. The stress reduction may result in a significant increase in the fatigue life of the component and, consequently, in the substantial reduction of the costs of repair or replacement of damaged and fractured components, providing customers with a reliable product at the lowest cost possible.

### 4. ACKNOWLEDGEMENTS

CNPq provided research scholarships, ABS Group do Brasil, specially his supervisor Viviane Krzonkalla, supported this work allowing research time for his employee, who received a tuition-free scholarship from PUC-Rio.

### 5. REFERENCES

- Castro, J.T.P. and Meggiolaro, M.A., 2009. *Fadiga técnicas e práticas de dimensionamento estrutural sob cargas reais de serviço, volume I: Iniciação de Trincas*, ISBN 1449514693, CreateSpace.
- Creager, M. and Paris, P.C., 1967. Elastic field equations for blunt cracks with reference to stress corrosion cracking. *International Journal of Fracture Mechanics*, v.3, p.247-252.
- Heller, M., Kaye, R. and Rose, L.R.F., 1999. A gradientless finite element procedure for shape optimization, *Journal of strain analysis*, vol. 34, No 5, pp. 323-336.
- Mattheck, C., 2006. Teacher tree: The evolution of notch shape optimization from complex to simple, *Engineering Fracture Mechanics*, vol. 73, No12, pp. 1732-1242.
- Mattheck, C.; Burkhardt, S., 1990. A new method of structural shape optimization based on biological growth, *International journal of fatigue*, vol. 12, No 3, pp. 185-190.
- Miranda, A.C.O., Meggiolaro, M.A., Castro, J.T.P., Martha, L.F., and Bittencourt, T.N., 2003. Fatigue life and crack path prediction in generic 2D structural components, *Engineering Fracture Mechanics* v.70, p.1259-79.
- Pilkey, W.D., 1997. *Peterson's stress concentration factors*, 2nd ed., Wiley.
- Taylor, D., Kelly, A., Toso, M., and Susmel, L., 2010. Two new methods for reducing stress concentration, *Engineering Failure Analysis*, available on line.
- Waldman, W., Heller, M., and Chen, G.X. 2000. Optimal free-form shapes for shoulder fillet in flat plates under tension and bending, *International Journal of Fatigue*, vol. 23, No 6, pp. 509-523.

### 6. RESPONSIBILITY NOTICE

The following text, properly adapted to the number of authors, must be included in the last section of the paper:  
The author(s) is (are) the only responsible for the printed material included in this paper.